

Primary studies of the microsecond pulsed glow discharge as an emission source using a conventional hollow cathode lamp[†]

Xiaomei Yan[‡], Wei Hang[‡], B. W. Smith, J. D. Winefordner and W. W. Harrison*

Department of Chemistry, University of Florida, Gainesville, FL32611, USA

Primary investigations on the operation of a glow discharge in the microsecond regime as an emission source have been carried out by using conventional hollow cathode lamps. By passing large currents of short duration repetitively through a conventional hollow cathode lamp, and making use of a gated detection system, light intensity enhancement of up to 3–4 orders of magnitude can be achieved with respect to dc operation. Intensity comparisons have been conducted on 4 hollow cathode lamps, As, Ca, Cu and Ti, for both the analyte and the filler gas species. The effects of variation of pulse conditions were examined in great detail on a Ti lamp. Temporally resolved voltage, current and emission profiles, with the analytical characteristics, demonstrate that microsecond pulsed operation does offer unique analytical advantages.

Keywords: Glow discharge; atomic emission spectrometry; hollow cathode lamp; microsecond pulse

The glow discharge (GD), as an effective excitation and ionization source, has enjoyed growing application for the direct analysis of major, minor and trace elements in solid materials.^{1,2} Most glow discharge systems operate with continuous direct current (dc) or radiofrequency (rf) mode to yield a steady-state plasma. However, the power applied to the glow discharge is 1–3 orders of magnitude smaller (several watts to tens of watts) with respect to the inductively coupled plasma (ICP) or microwave induced plasma (MIP) source. Higher GD power can lead to cathode sample overheating and plasma instability. At high powers, thermal sampling (arc or spark) can occur rather than sputtering sampling.³ To extend the glow discharge to a higher effective power level, a pulsed high current mode has been introduced.^{4,5}

In the pulsed mode, a reduced duty cycle permits the application of higher instantaneous power to generate an intensified signal, while the GD maintains an acceptably lower average power. Meanwhile, gated detection extracts time resolved information, not only for enhancing the analytical signal but also for diagnostic opportunities. In this way, the shorter the pulse and the lower the operating frequency, the more intense can be the pulse conditions. However, the majority of studies on the pulsed glow discharge published to date have been concentrated on the millisecond regime, where distinct benefits can be achieved compared with the conventional dc mode, but peak applied power is still limited.

With the development of today's instrumentation standards, interest has revived in the extension of pulsed glow discharge into the microsecond range. Hang *et al.*⁶ reported the coupling of a high-power, microsecond regime discharge to a time-of-flight mass spectrometer. Newly developed microsecond-pulsed TOFMS shows distinct advantages in high intensity and

temporal resolution between sample and gas species based on repeller delay setting.⁷ In our laboratory, special attention has been given to the employment of a microsecond discharge for glow discharge atomic emission,^{8–10} where several orders of magnitude signal improvement has been reported. The present study focuses in detail on the microsecond pulsed glow discharge employing a commercial hollow cathode lamp source.

Research on pulsed hollow cathode lamps can be found at least as far back as 30 years ago.¹¹ An extensive study concerning measurements of excitation, ionization and time dependence for a pulsed hollow cathode lamp has been published by Kielkopf.¹² By passing greater peak current through the lamps, significantly enhanced peak radiance can be attained. Typical values of two orders of magnitude increase in peak radiance of these lamps were observed.¹¹ Mitchell and Johansson^{13,14} originally applied the pulsed hollow cathode as a line source in an atomic fluorescence spectrometer for simultaneous multielement analysis. Later, Weide and Parsons¹⁵ showed approximately three orders of magnitude improvement in the limit of detection for zinc by using a pulsed system as opposed to a conventional dc system. Omenetto *et al.*¹⁶ reviewed the application of the pulsed hollow cathode lamp in fluorescence measurement. Moreover, the pulsed hollow cathode glow discharge also found temporal advantages in laser excited atomic fluorescence spectroscopy,¹⁷ wherein measurements were made 100 μ s after the discharge was extinguished.

Most of these early pulsed hollow cathode discharge studies concentrated on its use as a light source for AAS or AFS. Usually, relatively high duty cycles (high frequency, millisecond regime pulse) and constant dc bias current (several mA) were applied. Broadening and self-absorption were observed with resonance lines.^{18–20} In addition, the limited fast electronics inhibited the practical application of this pulsed technique at that time.

Though suffering from intrinsic complex emission spectra and two–three orders worse detection limits compared with mass spectrometry, glow discharge emission spectrometry still enjoys wide application in industry and laboratories, owing to its low cost, simplicity and an almost maintenance-free optical system. Encouraged by the potential sensitivity competitiveness of microsecond pulsed glow discharge emission with glow discharge mass spectrometry, we present here experimental studies at varied pulse conditions, as well as the electrical and spectroscopic characteristics of the microsecond operated hollow cathode lamps.

EXPERIMENTAL

Equipment

A schematic diagram of a microsecond pulsed glow discharge atomic emission system is illustrated in Fig. 1, where a commercial hollow cathode lamp (HCL) is used as the GD source. The HCL emission was focused 1:1 onto the entrance slit of the monochromator (Model 1680B, 0.22 m double

[†]Presented at the 1998 Winter Conference on Plasma Spectrochemistry, Scottsdale, AZ, USA, January 5–10, 1998.

[‡]Present address: Los Alamos National Laboratory, CST-9, MS K484, Los Alamos, NM 87545, USA.

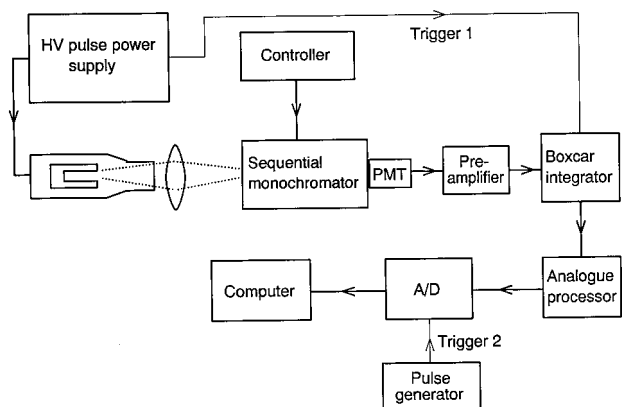


Fig. 1 Schematic diagram of microsecond pulsed hollow cathode lamp and detection system.

spectrometer, Spex, Edison, NJ, USA) by a biconvex fused silica lens. The slit width was set at 50 μm for both the entrance and the exit slit. This stepping motor controlled scanning monochromator has two 1200 gr mm^{-1} gratings and provides 0.2 nm resolution at 500 nm. The CD2A COMPUDRIVE communicates with the monochromator internal large stepper driver (LSD) through an RS-232 two-way interface.

A photomultiplier tube (Model R955, Hamamatsu, Bridgewater, NJ, USA) produced an output current that was converted to voltage by a small transimpedance amplifier (Model A-1, Thorn EMI, Gencom Inc., New York, USA). The signal was then processed with a gated integrator and boxcar averager (Model 250, Stanford Research Systems, Sunnyvale, CA, USA) in conjunction with an analogue processor (Model 235, Stanford Research Systems). All signals were digitized and sent to a computer *via* an analog-to-digital (A/D) converter (Model 245, Stanford Research Systems).

All four investigated hollow cathode lamps (neon filled), As (Model 14-386-104N, 10 torr), Ca (Model 14-386-100B, 6 torr), Cu (Model 14-386-100A, 5 torr) and Ti (Model 14-386-102H, 10 torr), were purchased from Fisher Scientific (Pittsburgh, PA, USA). If not otherwise mentioned, 900 V was applied to the PMT detector.

A high voltage pulse generator (Model 350, Velonex, Santa Clara, CA, USA) was employed to pulse the hollow cathode lamp in the microsecond range. This voltage regulated power supply provided pulse width and frequency variations from 0.1–300 μs and from 1–100 000 Hz, respectively, and voltage up to 3000 V could be applied to the cathode. No external trigger was necessary, as the power supply TTL output trigger was used to trigger the gated boxcar integrator. A separated pulse generator determines the independent A/D converter sampling rate.

Temporal profile recording

With the monochromator set at a specific wavelength, a temporal profile of the lamp emission was directly traced by a fast oscilloscope (Hewlett-Packard 54542C Digitizing Oscilloscope, 2 GSa s^{-1} , 500 MHz, Palo Alto, CA, USA). The output signal from the PMT was displayed on the oscilloscope simultaneously with discharge current and voltage (through a 1000:1 attenuator). The pulse current was determined by calculation from the peak voltage dropped across a 5.6 Ω carbon resistor.

Spectra collection

Using a scanning monochromator with photomultiplier detector for a pulsed source is not ideal. The most suitable detector would be some form of direct reader or image array detector

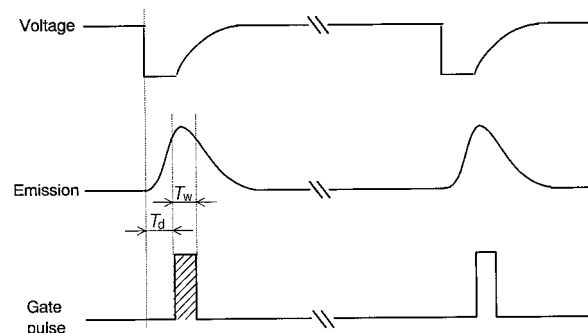


Fig. 2 Timing diagram of modulation pulse and gate pulse. t_d = Delay of signal gate; t_w = boxcar gate width.

with gating possibility, such as the intensified photodiode array (PDA), and intensified charge-coupled device (CCD) arrays. In that way, the advantages offered by the pulsed glow discharge emission source can be fully realized. However, limited by the present system, we have collected spectra in the following way.

The timing diagram of the system is given in Fig. 2. The pulsed power supply controls the repetition rate of the whole system. Its TTL output triggers the boxcar integrator, where a variable delay (T_d , 1 ns–10 ms) and width (T_w , 1 ns–15 ms) for the gate window are available. The delay of the window allows setting the interval between the onset of the lamp voltage pulse and the acquisition of emission. The utilization of the built-in average function of the boxcar integrator improves signal-to-noise ratio.

RESULTS AND DISCUSSION

Temporal emission profiles

Atomic emission profiles with respect to time, after pulse discharge initiation, were obtained for several key hollow cathode discharge species. We have compared both atom and ion emission signals from sputtered analyte species and from the discharge fill gas. In addition, current and voltage responses are illustrated for the pulse discharge period. Responses obtained from Ti and Cu hollow cathode lamps are shown in Figs. 3 (a) and (b), respectively. Typically, a 10 μs pulse was applied to the lamps at 200 Hz. Peak discharge currents can reach as high as 4 A, and peak powers of 1.4 kW for the Ti HCL and 1.8 kW for the Cu HCL can be achieved.

Current–voltage response

Applying high voltage does not immediately yield an emission signal, but several processes are set in motion. The first 50–100 ns show wide voltage fluctuations as the discharge begins to stabilize by breaking down the fill gas to produce a reliable source of charge carriers. The sharp decrease in plasma impedance causes a rapid increase in current and a drop in sustaining voltage. These responses vary from one hollow cathode lamp to another as a function of the cathode material, lamp configuration and discharge gas composition and pressure.

Emission response

Two different emission regimes might be expected. First, there are those species (discharge gas) that are available for excitation immediately upon discharge initiation. The second group of discharge species arises from the sputtered cathode material. For the latter, it is only after sputter ablation begins and sufficient numbers diffuse into the prime excitation zone that measurable emission response will be observed. For all the

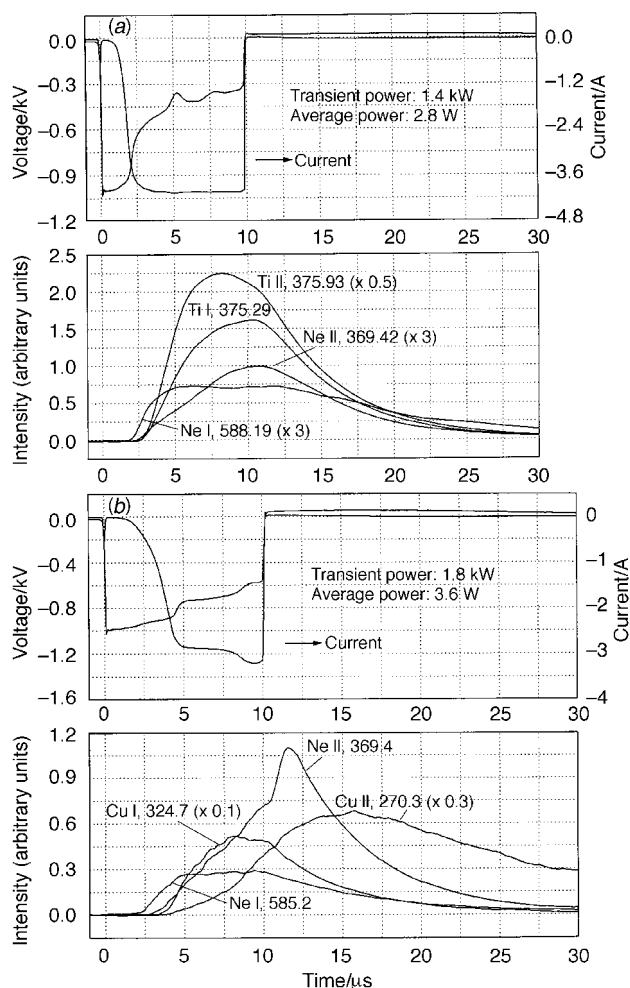


Fig. 3 Typical time-resolved profiles for pulsed mode hollow cathode lamps at 200 Hz. (a) Ti lamp; (b) Cu lamp.

available discharge species, their appearance and optimization will also depend on the energy of the discharge relative to the available spectroscopic energy levels of the atoms. All these considerations should produce a diversity of time profiles of fundamental interest and even potentially of analytical opportunity with proper time resolution.

As indicated in Fig. 3, neon atom excitation appears quickly following the discharge initiation. This is not surprising, since it fills the entire lamp body and is available for immediate excitation from the first electron current of sufficient energy. It achieves a maximum at about 5 μs after the onset of the voltage, maintains a plateau until the plasma shuts off, and then gradually decays for another 10–20 μs . Emission from neon ions (Ne II) occurs somewhat later in the discharge pulse and only peaks after the termination of the power supply peak. The slower rise time of the Ne II emission relative to the Ne I emission could arise from a two-step electron impact as the ionization mechanism in the fill gas, with Ne metastables as possible intermediates.^{21,22} The later formation of the neon ions, which are the primary sputter agents for the discharge, may have implications for the time response of the analyte atoms.

The emission response of the sputtered cathode atoms shows a different pattern compared with the discharge gas, and there is an obvious difference in response between copper and titanium in Fig. 3. A slight delay between cathode atom lines with respect to the Ne II emission reflects the time required for the cathode sputtering by Ne II ions, and the transport of the sputtered atoms into the negative region for subsequent excitation. We have examined temporal responses from Ti, Cu, As and Ca hollow cathode lamps.

For relatively low ionization potential (IP) elements, such as Ca (6.11 eV) and Ti (6.82 eV), almost no temporal difference between ionic and atomic lines can be observed [Ti, Fig. 3(a)]. On the other hand, Cu (7.73 eV) [Fig. 3(b)] and As (9.81 eV) ionic lines appear later in time and reach a maximum only after termination of the pulse. However, the higher ionization potential of As compared to Cu did not cause significant differentiation of its response, so other factors are also likely to be involved. More systematic studies of metal ionic emission in the discharge may help us better understand the ionization and excitation process for the analyte atoms.

Discharge parameters

An analysis of discharge characteristics was carried out by employing a Ti hollow cathode lamp. Variations of peak current, peak power, current delay and emission intensity as a function of initiation voltage are illustrated in Fig. 4. The left y-axis units are A, kW and μs for peak current, peak power and current delay, respectively. Emission response (right y-axis) from the Ti atom line (498.17 nm) was monitored, and peak height represents the maximum intensity during the overall pulse region. The position for peak current and peak power measurement was chosen just before the termination of the plasma (see Fig. 3). Current delay, defined as the interval between initiation and the rising edge of the current with respect to voltage, is estimated as the time at which current reaches 50% of maximum value.

As is shown in Fig. 4, with an increase in the initial voltage from 500 V to 1000 V, the current delay drops from 8.5 to 2 μs , reflecting the rapid build-up of current flow through the lamp at higher voltages. An intensified electric field creates a fast discharge breakdown, and an enhanced number density of charged particles. Both the peak current and peak power response curves follow a linear relationship with the initial voltage over the range shown in Fig. 4. Peak current increases from 1 A at 500 V to 3.8 A at 1000 V, while peak power rises from 0.4 to 2.7 kW. Compared with the limited current and power dissipation using a conventional dc glow discharge, with the pulsed microsecond mode up to 3 orders of magnitude enhancement can be achieved. Resulting emission intensity shows a corresponding large increase during the pulse 'on' region. Even for high intensity pulsing, the average discharge power can be kept even lower than that of the dc mode by controlling frequency or pulse width to reduce the duty cycle.

With regard to pulse operating frequency, in principle the lower the repetition rate, the higher the allowed voltage and current (average power = peak power \times duty cycle). But reduced frequency leads to a longer analysis time to accomplish

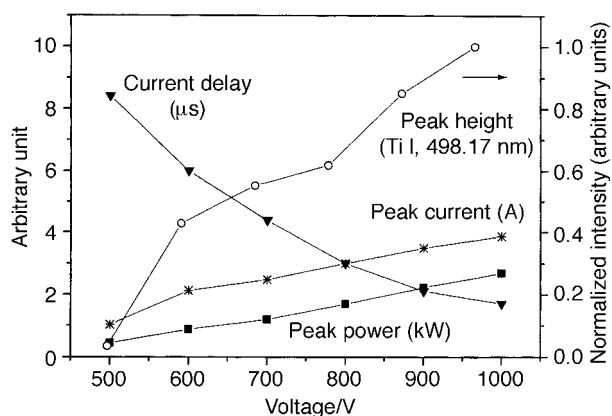


Fig. 4 Variation of peak current, peak power, peak power and current delay as a function of applied voltage on Ti hollow cathode lamp. Boxcar delay 7 μs , gate width 3 μs .

comparable signal averages or accumulation. Recent studies on microseconds-pulsed GD-TOF-MS²³ show that if a glow discharge is operated at very low frequency (e.g., 0.1 Hz), pulse width needs to be increased correspondingly for satisfactory plasma generation. Greater time between pulses also allows more redeposition and surface processes to occur that require removal with the next pulse. On the other hand, as pulses become more frequent, there is eventually not enough time between successive pulses to dissipate completely the sputtered atoms. The accumulation of absorbing atoms might cause self-absorption or self-reversal of resonance lines. Also, in such cases reduced current delay has been observed due to the residue ions from the previous pulse.

Self absorption

Any process that injects large numbers of analyte atoms into the discharge may lead to self absorption effects if diffusion processes are not able to keep the atom density below critical levels. This has been reported previously^{18,19} in studies of pulsed hollow cathode lamps in AAS and AFS. Since glow discharges involve cathode sputtering and subsequent excitation in the same discharge source, a compromise in atom population must always be considered between emission requirements on the one hand and self-absorption limitations on the other.

Time-resolved studies of the hyperfine lines of the Cu 324.7 nm transition have shown that self absorption starts from 4–21 μ s and self-reversal starts after about 50 μ s and reaches a steady state at about 200 μ s for a 10 Hz, 5 μ s and 200 mA pulse.¹⁸ Further results showed that self-reversal increases with repetition frequency, and lines exhibited broadening with increased current.²⁰ Operating the pulsed glow discharge in a fast pulse, low duty cycle mode, even at high currents, allows diffusion processes to reduce self absorption effects, although not completely.

The emission intensity ratio of the two major copper resonance lines (324.75 nm and 327.40 nm) should be close to 2 in the absence of self absorption. Since the Cu 324.75 nm line is more strongly absorbed than the 327.40 nm line,²⁴ large atom populations can reduce this ratio and serve as one measure of self-absorption and eventually self-reversal. Fig. 5 shows spectra acquired for copper resonance lines at dc and microsecond pulsed modes. For the dc mode, the emission intensity ratio of Cu 324.75 to Cu 327.40 nm was 2.0, which is similar to a previous report.²⁴ In the pulsed mode, the ratio decreased as a function of pulse frequency, as indicated from

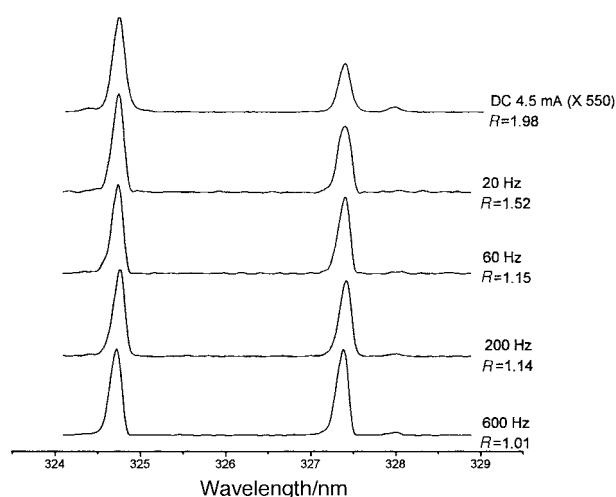


Fig. 5 Dependence of the intensity ratio of two Cu resonance lines on the hollow cathode lamp operating frequency.

the values shown for repetition rates from 20 to 600 Hz. These values indicate some level of self absorption, even at low frequencies, and at higher pulse rates the presence of residual absorbing atoms from the previous pulse produces greater self-absorption. Other studies indicated that at least several milliseconds of diffusion time is required to avoid self-absorption.⁸ Note that the hollow cathode lamps are closed systems, unlike the normal analytical glow discharge lamps that have a continual gas flow pattern that helps reduce this problem.

Suitable analytical conditions can also be found by adjusting the many variables provided by the pulsed operation mode (pulse amplitude, pulse width, repetition rate, boxcar delay time and gate width) to reduce or minimize self-absorption effects. There is also the opportunity in AES to choose from many spectral lines for optimum detection. With the significant intensity enhancement from the pulsed mode, some non-resonance lines will become much stronger compared with the dc mode and show utility. We do not believe the microsecond pulsed glow discharge will be limited by self absorption.

Emission spectra comparison

The major analytical advantage of the high current, short duration pulsed glow discharge is reflected in the high emission intensity. It is difficult to make direct comparisons of dc *versus* pulsed glow discharge intensities, since the measurement mode needs to be optimized for each. One approach is to set equivalent average power for both modes. However, average power in the pulsed mode can always be reduced by employing a lower repetition rate, while the emission intensity as read by a gated detection system is unaffected. For a realistic comparison, the conditions for measurement of emission intensity enhancement should be optimized in both the continuous dc and the microsecond pulsed modes.

Spectral comparisons were made with Ca, Ti, Cu and As hollow cathode lamps. For the Ca and Ti lamps, Table 1 shows atom and ion line emission data for the cathode metals and the neon fill gas. Selected lines in each spectrum are included, and the higher energy level for the transition is listed. Large intensity enhancements were observed for the atom lines, with even larger increases seen for the ion lines. The greater ionization shown for the plasma confirms its valuable role as a glow discharge ion source for mass spectrometry.⁷ In fact, the intensities observed in these studies for analyte ion lines give them utility as viable analysis lines by atomic emission spectroscopy as well.

A small comparison segment of the Ti hollow cathode emission spectrum is shown in Fig. 6. The dc spectrum [Fig. 6(a)] was obtained at 12 mA, 140 V, and the 10 μ s pulse emission spectrum [Fig. 6(b)] was taken at 200 Hz, 1.0 kV. By delaying the gate window, discriminated spectra can be obtained²⁵ based on the different temporal profile for every species. In this case, the boxcar delay was set at 7 μ s, and the gate window width was 3 μ s. The pulsed mode shows an intensity increase up to four orders of magnitude. As would be expected, the intensity of the background also increases, but to a much smaller extent than the intensity of the analytical lines. In keeping with the data in Table 1, Fig. 6 shows that the pulsed HCL is most favored for Ti II line enhancement compared with Ne II and Ti I lines, reflecting an efficient ionization of the sputtered atoms. In comparing full range spectra, we find some pulsed spectral lines that are not visible in the dc counterpart. More common are the differences in emission intensity ratios among various lines, indicating the differential population of energy levels between the two discharge modes.

The intensity enhancements for all four hollow cathode lamps studied follow the same general pattern: metal ionic lines increase most, metal atomic lines next, followed by inert gas ionic lines, and the fill gas atomic lines. The large

Table 1 Comparison of emission intensity between dc and μ s-pulsed hollow cathode lamps (Ca and Ti)

Ca* (6.11 eV)	Excitation energy/cm ⁻¹	Signal enhancement	Ti† (6.82 eV)	Excitation energy/cm ⁻¹	Signal enhancement
Ca I, 422.67	23 652	1757	Ti I, 364.27	27 615	980
Ca I, 430.25	38 552	3369	Ti I, 365.46	27 355	1200
Ca I, 443.50	37 752	3228	Ti I, 365.81	27 499	1580
Ca I, 445.48	37 757	2628	Ti I, 366.90	27 418	890
Ca II, 370.60	52 167	51 250	Ti II, 323.45	31 301	33 770
Ca II, 373.69	52 167	10 961	Ti II, 323.66	31 114	31 180
Ca II, 393.37	25 414	31 636	Ti II, 323.90	30 959	36 530
Ca II, 396.85	25 192	50 939	Ti II, 326.16	45 909	81 930
Ne I, 585.25	152 973	8	Ne I, 585.25		10
Ne I, 588.19	151 040	22	Ne I, 588.19		25
Ne II, 366.41	246 417	717	Ne II, 366.41		1005
Ne II, 369.42	246 195	484	Ne II, 369.42		660

* dc: 4.5 mA. Pulse: 10 μ s, 200 Hz, 0.8 kV. Boxcar: delay 7 μ s, window 3 μ s. † dc: 12 mA. Pulse: 10 μ s, 200 Hz, 1.0 kV. Boxcar: delay 7 μ s, window 3 μ s.

discrimination for the intensity increase of analyte species with respect to that of the rare gas is obviously an advantage in spectroscopic investigations. For analyte lines at least three orders of magnitude intensity improvement can be easily achieved, an effect due not only to the enhanced sputtering during the high current pulse but also to a more efficient excitation and ionization.

Different intensity enhancements are found for different lines. As shown in Table 1, Ti II (326.16 nm) has a much higher relative increase than the other three Ti II lines, which may be due to its higher excitation energy. But for Ca II (370.60 nm) and Ca II (373.69 nm) lines, though the transitions involve the same excitation level (52 167 cm⁻¹), there exists about a 5-fold enhancement difference. A more detailed investigation of additional elements and associated energy levels will be necessary to gain a better understanding of the plasma phenomena. For copper, the 324.75 and 327.40 nm resonance lines exhibit one order lower increase with respect to two non-

resonance lines, which could result from the self-absorption of sputtered atoms, undetectable with our system.

Though it is recognized that local thermal equilibrium (LTE) does not likely exist during this 10 μ s high current pulse, it is of some interest to calculate the 'apparent' ionization ratio of Ca atoms by means of eqn. (1):

$$\frac{N^+}{N^0} = \frac{(I\lambda)^+}{(I\lambda)^0} \frac{Z^+}{Z^0} \frac{(gA)^0}{(gA)^+} e^{\frac{E^+ - E^0}{kT}} \quad (1)$$

where N is the particle density, I the emission intensity, λ the wavelength of the line, Z the partition function, g the statistical weight of the upper level, A the Einstein transition probability, E the excitation energy, k the Boltzmann constant and T the absolute temperature of a source that follows a Boltzmann distribution of energy. The factors pertaining to the neutral atom and ion are designated by the superscripts 0 and $^+$, respectively. The temperature in the exponential term of the

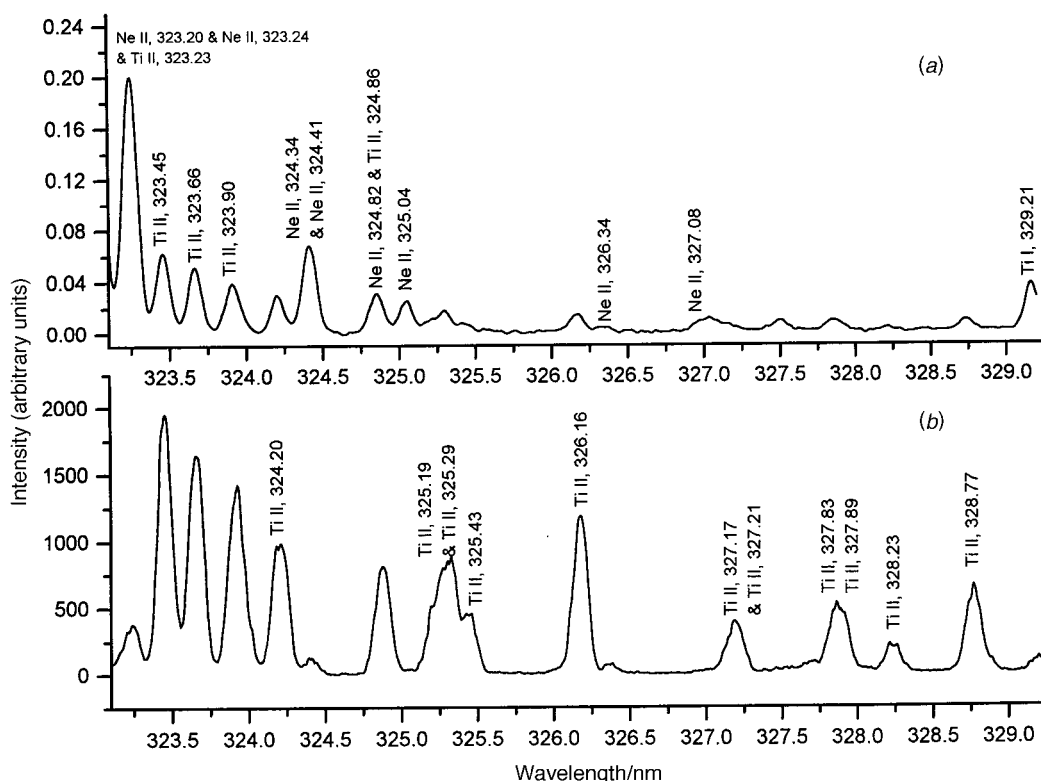


Fig. 6 Comparison of Ti emission spectra between dc and microsecond pulsed mode: (a), dc, 12 mA, 140 V; (b), 10 μ s, 200 Hz; initial voltage 1.0 kV, peak current 4.0 A, Boxcar delay 7 μ s, gate width 3 μ s.

Table 2 Comparison of analytical characteristics between dc and μ s-pulsed Ti hollow cathode lamp

Boxcar average	Signal* (dc)	RSD (%) (dc)	Signal (pulse)	RSD (%) (pulse)	Signal enhancement (pulse/dc)		
1	0.040	346	1302	36	32 550		
10	0.039	109	1344	10	34 461		
100	0.039	40	1301	3.8	33 359		
1000	0.039	9.7	1309	0.63	33 564		
Boxcar average	BG (dc)	BG noise (dc)	BG (pulse)	BG noise (pulse)	S/N (dc)	S/N (pulse)	S/N enhancement (pulse/dc)
1	0.002	0.021	1.052	0.720	1.9	1809	967
10	0.001	0.017	0.997	0.220	2.3	6121	2661
100	0.001	0.005	1.007	0.072	7.3	18 093	2479
1000	0.004	0.002	1.011	0.012	18.6	105 565	5676

* Signal was obtained at Ti II, 323.5 nm. Boxcar integrator delay 7 μ s, gate width 3 μ s. Operation condition: dc (12 mA, 140 V), pulse (10 μ s, 200 Hz, initial voltage 1.0 kV, peak current 4.0 A).

upper equation was determined by a two point Boltzmann plot, with the results of 4800 and 5600 K for the dc and pulsed modes, respectively. On this basis, but recalling the equilibrium *caveat* expressed above, the calculated ionization shows an increase from 4% in the dc mode to 71% in the pulsed mode. It is seen from the spectra that the pulsed discharge is much more highly ionized than its dc counterpart, and the calculations, while not to be taken quantitatively, support the direction of enhanced ionization.

Signal to noise ratio

The important point for analytical considerations is not the enhancement of raw intensity, but the improvement of detection limits, which is directly related to signal to background noise ratio. A comparison was made between the dc and microsecond pulsed modes using a Ti hollow cathode lamp. In order to study the signal properties with a common readout mode, the signals from the PMT detector were directed into a boxcar integrator without use of any analog or digital filtering for both dc and pulsed operation. A titanium ion line at 323.5 nm was selected as the analyte spectral line for signal monitoring. The background value was measured at 367.5 nm, where no elemental emission was observed. The signal intensity, relative standard deviation (RSD) of the signal, background, background noise, signal to background noise ratio, and the enhancements for both pulsed and dc signal to noise ratio are listed in Table 2.

The large fluctuation for dc signals at small boxcar averaging times arises because no time constant has been used in the detection system. As the number of boxcar average times increased from 1 to 1000, the noise for both the dc and pulsed signal decreased, as reflected in the RSD improvement. Raw signal enhancement reaches four orders of magnitude. Though the background level also increases, this increase is more modest, leading to an attractive enhancement of the signal to background noise (S/N) ratio. Generally, about three orders of magnitude of S/N enhancement can be consistently obtained.

CONCLUSION

The application of high current, short duration pulses to hollow cathode lamps shows several interesting advantages. The instantaneous power can be higher than 1 kW, which approaches the power of an ICP. Signal to noise ratio improves up to 3 orders of magnitude for some ionic lines. A much higher increase in ion lines demonstrates a more energetic plasma generated in the pulsed mode. In order to determine the full potential of the pulsed glow discharge, much in the way of plasma diagnostics remains to be done, such as number density studies of electrons and metastable argon atoms during and after the pulse. The large increase in pulsed plasma

ionization suggests the opportunity for ion emission lines in atomic emission and also enhanced value as an ion source for mass spectrometry.

This work was supported by a grant from the Department of Energy, Basic Energy Sciences, for which we are most grateful.

REFERENCES

- Harrison, W. W., Hess, K. R., Marcus, R. K., and King, F. L., *Anal. Chem.*, 1986, **58**, 341A.
- Marcus, R. K., *Glow Discharge Spectroscopies*, Plenum Press, New York, USA, 1993.
- Harrison, W. W., and Hang, W., *Fresenius J. Anal. Chem.*, 1996, **355**, 803.
- Klingler, J. A., Savickas, P. J., and Harrison, W. W., *J. Am. Soc. Mass Spectrom.*, 1990, **1**, 138.
- Pan, P., and King, F. L., *Anal. Chem.*, 1993, **65**, 3187.
- Hang, W., Yang, P., Wang, X., Yang, C., Su, Y., and Huang, B., *Rapid Commun. Mass Spectrom.*, 1994, **8**, 590.
- Hang, W., and Harrison, W. W., *J. Anal. At. Spectrom.*, 1996, **11**, 835.
- Walden, W. O., Hang, W., Smith, B. W., Winefordner, J. D., and Harrison, W. W., *Fresenius J. Anal. Chem.*, 1996, **355**, 442.
- Hang, W., Walden, W. O., and Harrison, W. W., *Anal. Chem.*, 1996, **68**, 1148.
- Pollmann, D., Ingeneri, K., and Harrison, W. W., *J. Anal. At. Spectrom.*, 1996, **11**, 849.
- Dawson, J. B., and Ellis, D. J., *Spectrochim. Acta, Part A*, 1967, **23**, 565.
- Kielkopf, J. F., *Spectrochim. Acta, Part B*, 1971, **26**, 371.
- Mitchell, D. G., and Johansson, A., *Spectrochim. Acta, Part B*, 1970, **25**, 175.
- Mitchell, D. G., and Johansson, A., *Spectrochim. Acta, Part B*, 1971, **26**, 677.
- Weide, J. O., and Parsons, M. L., *Anal. Lett.*, 1972, **5**, 363.
- Omenetto, N., Fraser, L. M., and Winefordner, J. D., *Appl. Spectrosc. Rev.*, 1973, **7**, 147.
- Glick, M., Smith, B. W., and Winefordner, J. D., *Anal. Chem.*, 1990, **62**, 157.
- Dejind, G. J., and Piepmeier, E. H., *Anal. Chem.*, 1974, **46**, 318.
- Dejind, G. J., and Piepmeier, E. H., *Spectrochim. Acta, Part B*, 1974, **29**, 159.
- Piepmeier, E. H., and de Galan, L., *Spectrochim. Acta, Part B*, 1975, **30**, 263.
- Farnsworth, P. B., and Walters, J. P., *Spectrochim. Acta, Part B*, 1982, **37**, 773.
- Strauss, J. A., Ferreira, N. P., and Human, H. G. C., *Spectrochim. Acta, Part B*, 1982, **37**, 947.
- Hang, W., and Harrison, W. W., to be published.
- Patel, B. M., and Winefordner, J. D., *Can. J. Spectrosc.*, 1987, **32**, 138.
- Harrison, W. W., Hang, W., Yan, X., Ingeneri, K., and Shelling, C., *J. Anal. At. Spectrom.*, 1997, **12**, 891.

Paper 8/02393J

Received March 30, 1998

Accepted July 16, 1998